Eurographics Symposium on Rendering 2017
P. Sander and M. Zwicker
(Guest Editors)

Volume 36 (2017), Number 4

Variance and Convergence Analysis of Monte Carlo Line and Segment Sampling Supplementary Material

Gurprit Singh Bailey Miller Wojciech Jarosz

Dartmouth College

In this document, we provide additional proofs and results to support the theory presented in the main paper.

1. Additive expected power spectra

If we have two uncorrelated random variables (MC line estimators in different directions using uncorrelated sample locations), then their variances are additive. To mathematically represent the same in the Fourier domain, we start by rewriting the Monte Carlo estimator as a weighted sum of estimators over all m directions:

$$I_N = \sum_{k=1}^{m} \frac{N_k}{N} I_{N_k} \tag{1}$$

$$I_N = \int_{\mathbb{D}} P_N(\mathbf{x}) f(\mathbf{x}) \mathrm{d}x = \int_{\mathbb{D}} \sum_{k=1}^{m} \frac{N_k}{N} P_{N_k}(\mathbf{x}) f(\mathbf{x}) \mathrm{d}x \tag{2}$$

where P_{N_k} is a sampling function along the k-th direction for N_k samples and $N = \sum_{k=1}^{m} N_k$ and N_k. This also let us write the sampling function as:

$$P_N(\mathbf{x}) = \sum_{k=1}^{m} \frac{N_k}{N} P_{N_k}(\mathbf{x}) \tag{3}$$

If we take the Fourier transform of this sampling function, then by using the linearity property of the Fourier transform we get:

$$\mathcal{F}_{P_N}(\nu) = \sum_{k=1}^{m} \frac{N_k}{N} \mathcal{F}_{P_{N_k}}(\nu) \tag{4}$$

Following the variance formulation from Eq. (4), from the main paper, we would like to obtain the power spectrum of P_N—which is a weighted sum of sampling functions P_{N_k}—to write the variance. We here claim that for *uncorrelated* random variables, we can write the expected power spectrum of a sum of random variables as a (weighted) sum of individual power spectra. In our case, for *uncorrelated* multiple directions, we can write the expected line sampling power spectrum as a weighted sum of power spectra along each individual direction, that is:

$$\langle \mathcal{P}_{P_N}(\nu) \rangle = \frac{N_k^2}{N^2} \langle \mathcal{P}_{P_{N_k}}(\nu) \rangle \tag{5}$$

Proof: We rely on the property that: *the autocorrelation ($R(\tau)$) of the sum of two completely uncorrelated functions (the cross-correlation is zero over all τ) is the sum of the autocorrelations of each function separately*. Let us denote any two uncorrelated (random variables) functions as $g_1(\cdot)$ and $g_2(\cdot)$, such that, the autocorrelation of the sum of these two functions can be written as:

$$R_{g_1+g_2}(\tau) = R_{g_1}(\tau) + R_{g_2}(\tau) \tag{6}$$

Using the addition theorem [Bra00], the Fourier transform of the sum of two such functions can be written as:

$$\mathcal{F}_{g_1+g_2}(\nu) = \mathcal{F}_{g_1}(\nu) + \mathcal{F}_{g_2}(\nu) \tag{7}$$

which implies that if we take the Fourier transform of (6), we obtain:

$$\mathcal{F}_{R_{g_1+g_2}}(\nu) = \mathcal{F}_{R_{g_1}}(\nu) + \mathcal{F}_{R_{g_2}}(\nu)\,. \tag{8}$$

Since the power spectrum ($\mathcal{P}$) of any function $g(\cdot)$ is equivalent to the Fourier transform ($\mathcal{F}$) of the autocorrelation of $g(\cdot)$ (autocorrelation theorem [Bra00]), we can write:

$$\mathcal{P}g(\nu) = \mathcal{F}_{R_g}(\nu), \tag{9}$$

$$\mathcal{P}g_1 + g_2(\nu) = \mathcal{F}_{R_{g_1+g_2}}(\nu). \tag{10}$$

Using (8), we can rewrite above equation as:

$$\mathcal{P}g_1 + g_2(\nu) = \mathcal{F}_{R_{g_1}}(\nu) + \mathcal{F}_{R_{g_2}}(\nu). \tag{11}$$

Using (9):

$$\mathcal{P}g_1 + g_2(\nu) = \mathcal{P}g_1(\nu) + \mathcal{P}g_2(\nu) \tag{12}$$

By taking the expected mean $\langle \cdot \rangle$ of the above equation, we obtain:

$$\langle \mathcal{P}g_1 + g_2(\nu) \rangle = \langle \mathcal{P}g_1(\nu) + \mathcal{P}g_2(\nu) \rangle \tag{13}$$

$$= \langle \mathcal{P}g_1(\nu) \rangle + \langle \mathcal{P}g_2(\nu) \rangle\,, \tag{14}$$

where we use the linearity property of the expectation operator. This shows that the expected power spectra of two uncorrelated variables (functions) can be added. In our case, the expected power spectra in multiple directions can be added together to obtained the expected power spectrum of all the directions together, given that all directions are generated in an uncorrelated fashion. Any scaling factor associated to the Fourier spectrum gets squared while computing the power spectrum which explains the N_k^2/N^2 factor in (5) and in the main paper (Eqs. 16 and 17). □

2. Theoretical convergence analysis

In the main paper, to derive theoretical convergence rates we restrict our integrands to integrable functions of the form $f(x)\chi_\Omega(x)$ with $f(x)$ is defined in Ω, a bounded domain, with smooth boundary (where $\chi_\Omega(x)$ is a characteristic function of Ω) [BCT01]. This can, however, be extended to arbitrary bounded convex regions [BHI03]. The worst case from this class of functions exhibits the power fall-off of the order $\mathcal{O}\left(\rho^{-(d+1)}\right)$ where $\rho > 0$ is a radial frequency.

Best and Worse case: To obtain the best and worse case convergence rate for various samplers we first fix our integrand power spectrum $\mathcal{P}_f(\rho\mathbf{n}_k)$, along each direction $\mathbf{n}_k$, to have the form:

$$\mathcal{P}_f^B(\rho\mathbf{n}_k) = \begin{cases} c_f & \rho < \rho_0, \\ 0 & \text{otherwise.}, \end{cases} \text{and} \, \mathcal{P}_f^W(\rho\mathbf{n}_k) = \begin{cases} c_f & \rho < \rho_0, \\ c_f\rho^{-d-1} & \text{otherwise} \end{cases} \tag{15}$$

where $\mathcal{P}_f^B$ represents the best case power spectrum, $\mathcal{P}_f^W$ power spectrum, $c_f > 0$ is a constant and $\rho_0 \in \mathbb{R}^+/0$ is finite. Note that, in the main paper we may drop the superscripts for brevity and refer implicitly to the case (best or worst) we are studying. These worst and best case defintions are used to analytically derive convergence rates for different sampling patterns by Pilleboue et al. [PSC*15].

References

[BCT01] BRANDOLINI L., COLZANI L., TORLASCHI A.: Mean square decay of Fourier transforms in Euclidean and non Euclidean spaces. *Tohoku Math. J. (2) 53*, 3 (2001), 467–478. doi:10.2748/tmj/1178207421. 2

[BHI03] BRANDOLINI L., HOFMANN S., IOSEVICH A.: Sharp rate of average decay of the Fourier transform of a bounded set. *Geometric & Functional Analysis GAFA 13*, 4 (2003), 671–680. 2

[Bra00] BRACEWELL R.: *The Fourier Transform and Its Applications*. Electrical engineering series. McGraw Hill, 2000. 1

[PSC*15] PILLEBOUE A., SINGH G., COEURJOLLY D., KAZHDAN M., OSTROMOUKHOV V.: Variance analysis for Monte Carlo integration. *ACM Transaction on Graphics (SIGGRAPH) 34*, 4 (July 2015), 124:1–124:14. doi:10.1145/2766930. 2

[SJ17] SINGH G., JAROSZ W.: Convergence analysis for anisotropic Monte Carlo sampling spectra. *ACM Transaction on Graphics (SIGGRAPH) 36*, 4 (July 2017), 137:1–137:14. doi:10.1145/3072959.3073656. 4

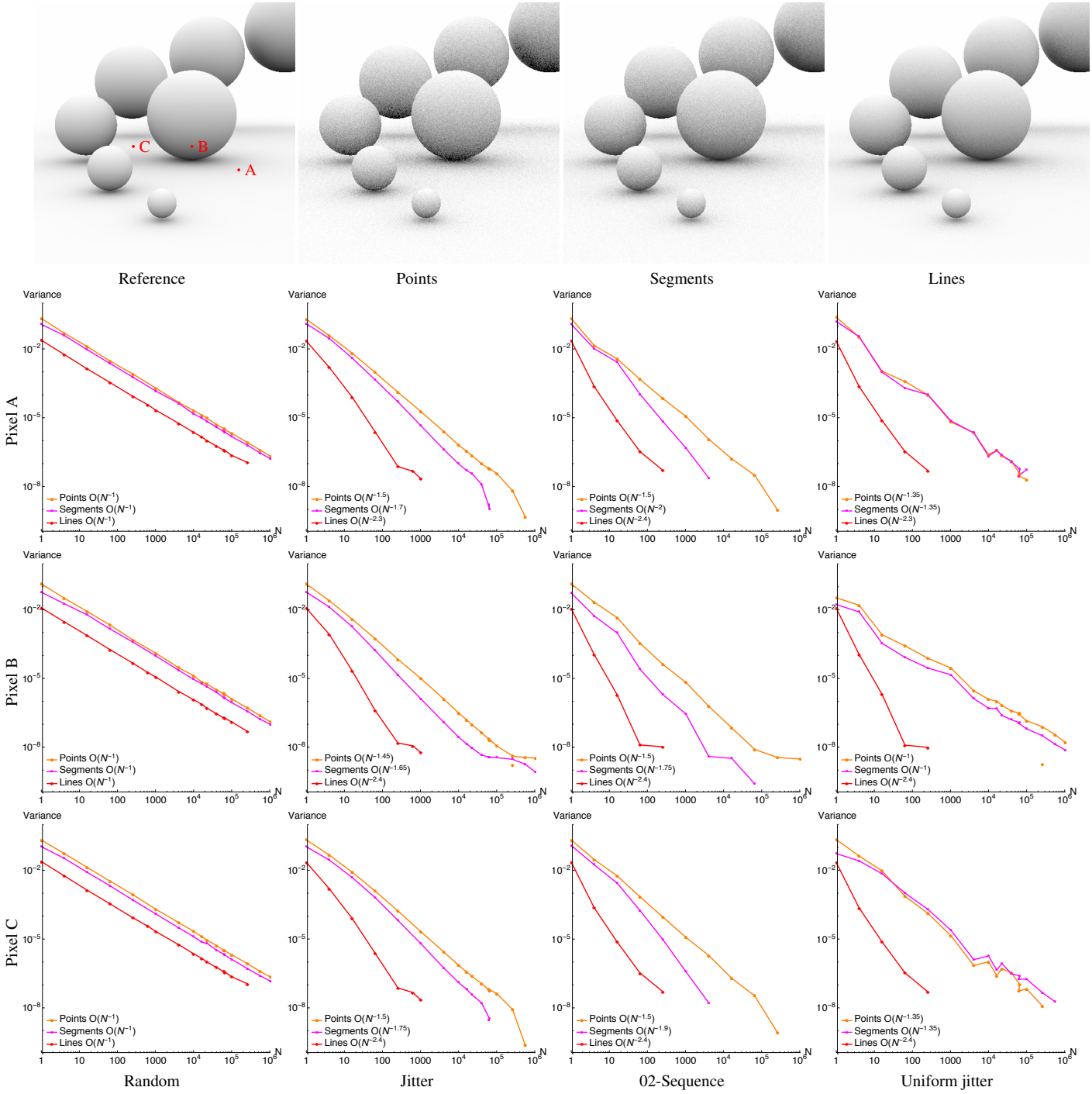

Figure 1: ***Points, Segments & Lines:*** *The ambient occlusion rendered with points, segments (of length=1 radian) and line samples in the top row. The reference is generated with $N = 1024$ line samples, the other images in the first row are generated with $N = 4$ samples. The bottom row illustrates the impact of segments and lines over point samples on the convergence rate for Pixel A marked in red.*

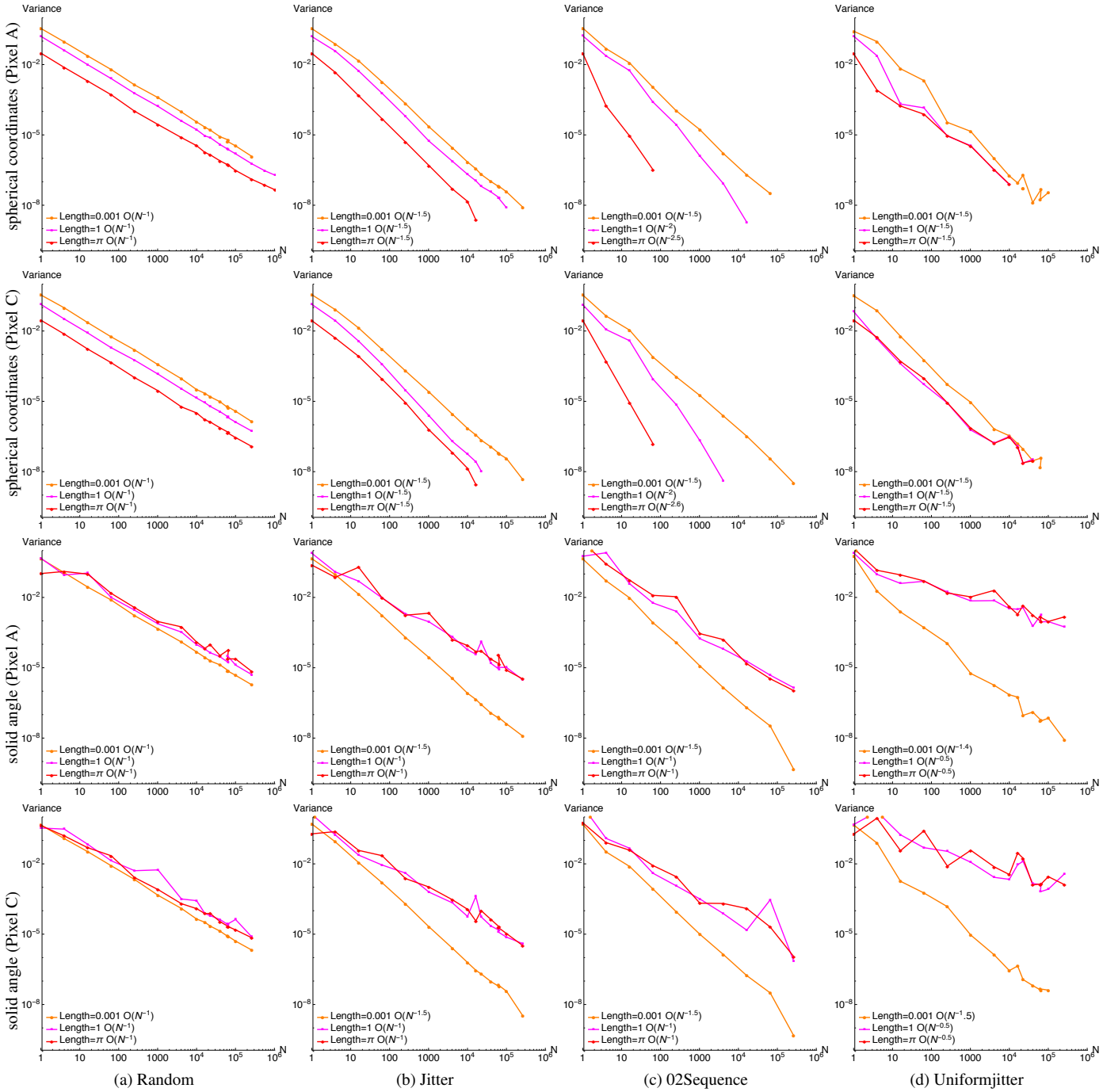

(a) Random (b) Jitter (c) 02Sequence (d) Uniformjitter

Figure 2: ***Segment sampling (Pixel A):*** *We compare the impact of segment lengths on the variance convergence rates while performing MC integration using segment samples for the ambient occlusion scene from the main paper (Fig.7).* ***Top two rows:*** *Increasing the length of segments does not affect the overall convergence for random and jittered samples. However, for 02Sequence sampler segment samples the convergence rate is improving with the increase in length and with length = π (which is equivalent to line sample) it behaves exactly like line samples. This can be explained from the fact that 02Sequence sampler has denser stratification in both 1D and 2D. As a result, segments restrict the integrand energy more in the horizontal direction, thereby, aligning the integrand spectrum anisotropy more closely to the sampling spectrum anisotropy [SJ17].* ***Bottom two rows:*** *When sampling with uniform solid angle or cosine weighted solid angle, the fireflies introduced due to the* $\sin\theta$ *and* $\cos\theta$ *terms in the MC estimator (see Eq. 25 in the main paper) makes the variance go haywire for long segments, however, with small segments the* $\sin\theta$ *and* $\cos\theta$ *terms still balance the numerator terms thereby converging without any kinks in the plots.*

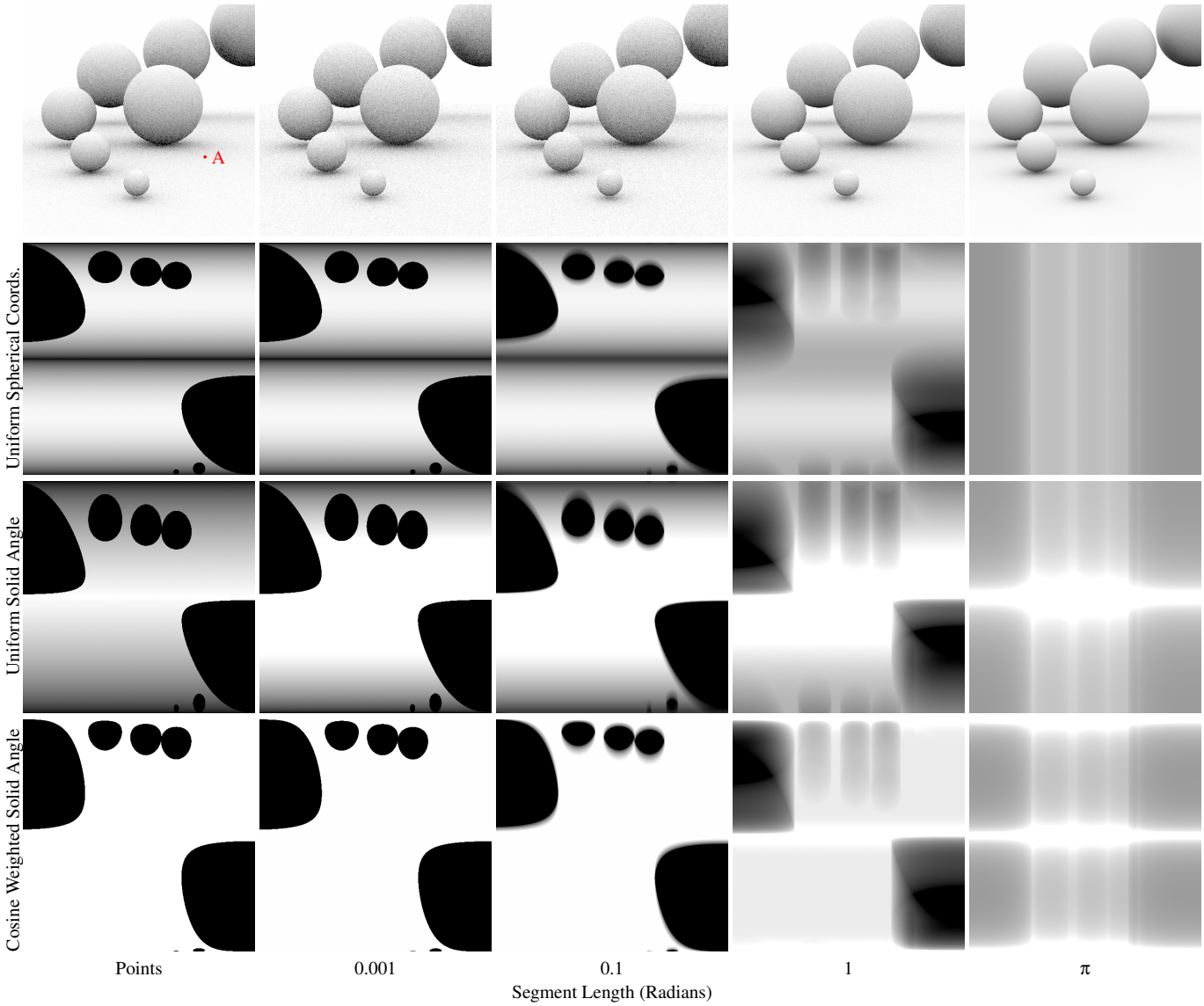

Figure 3: ***Visualizing Monte Carlo estimator for individual pixel with line segment sampling:*** *In the top row, the renderings are generated with $N = 9$ jittered samples. The Monte Carlo estimator (Eq. 25 of the main paper) for pixel A is computed for point and segment samples from various distributions and visualized in random number space $[0,1)^2$. The vertical axis correspond to $\theta \in [-\pi/2, \pi/2)$ and the horizontal axis correspond to $\phi \in [0, \pi)$ in spherical coordinates. As the line segment length increases from 0.001 radians to π radians, the integral gets pre-filtered with segment samples and tend to be a 1D function. At a segment length of π, the integral becomes 1D function but only with uniform spherical coordinate sampling for which the pdf is a constant term. For other pdfs (bottom two rows) we do not observe a 1D function since the $\sin\theta$ term (in the case of uniform solid angle) and the $\cos\theta\sin\theta$ term (in the case of cosine weighted solid angle) in these pdfs—unlike point samples—does not cancel out in Eq.25 of the main paper.*

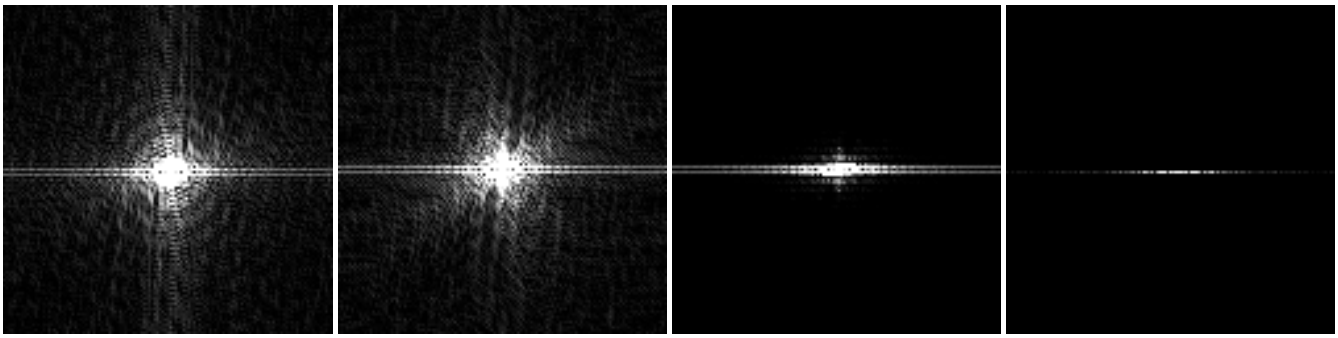

(a) Points (b) $l = 0.001$ (c) $l = 1$ (d) $l = \pi$

Figure 4: ***Segment sampling spectra (Pixel A):*** *Fourier power spectrum computed with 16384 regular grid samples for integrand underneath Pixel A for point samples in (a) and for segments with different length in (b,c,d). Since the integrand is convolved verrtically with finite length segment samples the power spectrum varies less and less vertically with an increase segment length and becomes 1D for* $l = \pi$.

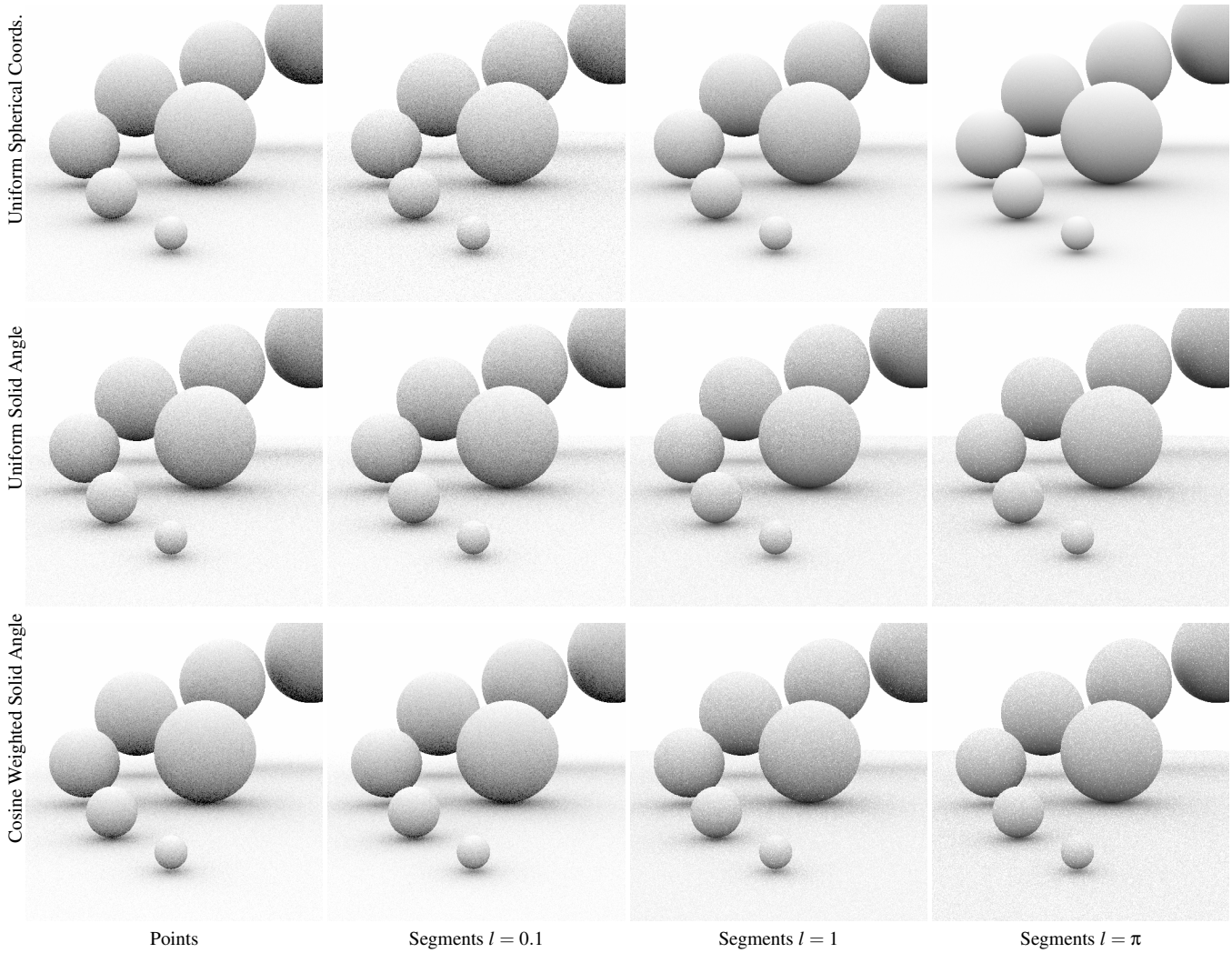

Figure 5: ***Visualizing fireflies for line segment sampling:*** *Above we show our scene rendered with various sampling methods. Observe that for uniform solid angle sampling and the cosine weighted solid angle sampling, the rendering contains fireflies. This is a result of the effects of the* sin *and* cos *terms in the denominator of the Monte Carlo estimator (Eq. 25 in the main paper) which doesn't cancel out with the numerator for segments. We also visualize the integrand underneath Pixel A in Fig. 3 to further analyze these fireflies.*